Influence of PMMA-Chain-End Tethered Polyhedral Oligomeric Silsesquioxanes on the Miscibility and Specific Interaction with Phenolic Blends

Chih-Feng Huang,[†] Shiao-Wei Kuo,*[,†] Fang-Ju Lin,[†] Wu-Jang Huang,[‡] Chih-Feng Wang,[†] Wen-Yi Chen,[§] and Feng-Chih Chang[†]

Institute of Applied Chemistry, National Chiao Tung University, Hsin Chu, Taiwan; Department of Environmental Science and Engineering, National Ping-Tung University of Science and Technology, Ping-Tung, Taiwan; and Department of Chemical Engineering, Yunlin University of Science and Technology, Yunlin 640, Taiwan

Received September 4, 2005; Revised Manuscript Received October 26, 2005

ABSTRACT: Two different molecular weights of poly(methyl methacrylate) (PMMA) and PMMA containing polyhedral oligomeric silsesquioxane (PMMA−POSS) homopolymers have been prepared via the atom transfer radical polymerization (ATRP) technique. The miscibility and specific interaction behaviors of PMMA−POSS and PMMA with phenolic resin were investigated by differential scanning calorimetry and Fourier transform infrared spectroscopy (FTIR). FTIR results reveal that at least three competing equilibriums are present in the phenolic/PMMA−POSS blend: self-association of phenolic (hydroxyl−hydroxyl), hydroxyl−siloxane interassociation between phenolic and POSS, and hydroxyl−carbonyl interassociation between phenolic and PMMA. Among these blends, single and higher T_gs of these phenolic/PMMA−POSS blends were observed than the corresponding phenolic/PMMA blends at same composition, revealing that a stronger interassociation interaction of hydroxyl−siloxane than the hydroxyl−carbonyl interaction. Furthermore, we also found the screening effect in phenolic/LPMMA−POSS blends that tends to significantly decrease the hydrogen bond formation of the hydroxyl−carbonyl interassociation.

Introduction

Recently, investigation of nanocomposites based on the hybridization of inorganic materials and organic polymers on a molecular scale has increased dramatically with the rapid growth of nanoscale technologies.[1] Nanocomposites, combining the important properties from inorganic materials and organic polymers, can create new unique properties such as high gas barrier,[2] solvent resistance,[3] flame resistance properties, and so on. Polyhedral oligomeric silsesquioxane (POSS) is a new type of material capable of forming various nanocomposites. Properties of POSS are unique since one or more of the organic groups can be functionalized for polymerization, while the remaining unreactive groups are able to solubilize the inorganic core and allow for control over the interfacial interactions occurring between the POSS and the polymer matrix. POSS units can be incorporated into virtually all types of polymers either by blending,[4,5] grafting, or copolymerization reactions[6−9] and results in enhancements on polymer properties, such as increased thermal stability, reduced flammability, and dielectric constant. Because of their advantageous performance relative to the nonhybrid counterparts, POSS−polymer hybrid materials have attracted great interest recently.[10−18]

Phenolic/poly(methyl methacrylate) blend is a well-known example of the miscible blend system, and the nature of phase behavior and miscibility in phenolic/PMMA blends have been extensively studied.[19,20] The miscibility of polymer blends is commonly ascertained through the measurements of glass transition temperatures (T_g) by differential scanning calorimetry (DSC). Moreover, FT-IR and NMR spectroscopies are also powerful tools for characterizing detailed structures of polymers and their specific interactions because these features affect local electron densities and resulted in frequency shifts.[21−24] Recently, two-dimensional infrared (2D-IR) correlation spectroscopy has been applied widely in polymer science.[25−27] This novel method is able to detect the specific interactions between polymer chains by treating the spectral fluctuations as a function of perturbation, such as time, temperature, pressure, and composition. 2D-IR correlation spectroscopy is able to differentiate intra- and intermolecular interactions through the analysis of selected bands from the one-dimensional vibration spectrum.[28,29]

In this article, we would like to extend our previous study[4,19,30,31] to the inorganic−organic polymer hybrids involving a POSS moiety at the chain end synthesized by atom transfer radical polymerization (ATRP), which has been shown to be a versatile technique for the controlled polymerization of many monomers since 1995.[32−34] These well-defined PMMA and PMMA−POSS homopolymers were prepared via ATRP with designed molecular weights (ca. 1×10^4 and 3×10^4 g/mol). Both PMMA−POSS and PMMA were then blended with phenolic resin. It is of particular interest to see the POSS chain-end effect on thermal properties, miscibility behavior, and hydrogen-bonding interactions of the phenolic/PMMA blends.

Experimental Section

Materials and Syntheses of the POSS-Cl Initiator. Isobutyltrisilanol-POSS was obtain from Hybrid Plastics Co. and was used as received. Methyl methacrylate (MMA) monomer was distilled from the calcium hydride and stored under N_2. Copper(I) bromide (CuBr) was purified by washing with glacial acetic acid overnight, followed by absolute ethanol and ethyl ether, and then dried under vacuum. Amberlite IR-120 (H form) cation-exchange resin, anisole, *N*,*N*,*N*′,*N*″,*N*″-pentamethyldiethylenetriamine (PMDETA), methyl

[†] National Chiao Tung University.
[‡] National Ping-Tung University of Science and Technology.
[§] Yunlin University of Science and Technology.
* To whom correspondence should be addressed.

10.1021/ma051923n CCC: $33.50
Published on Web 12/13/2005

Scheme 1. Synthetic Route To Prepare PMMA−POSS and PMMA Polymers

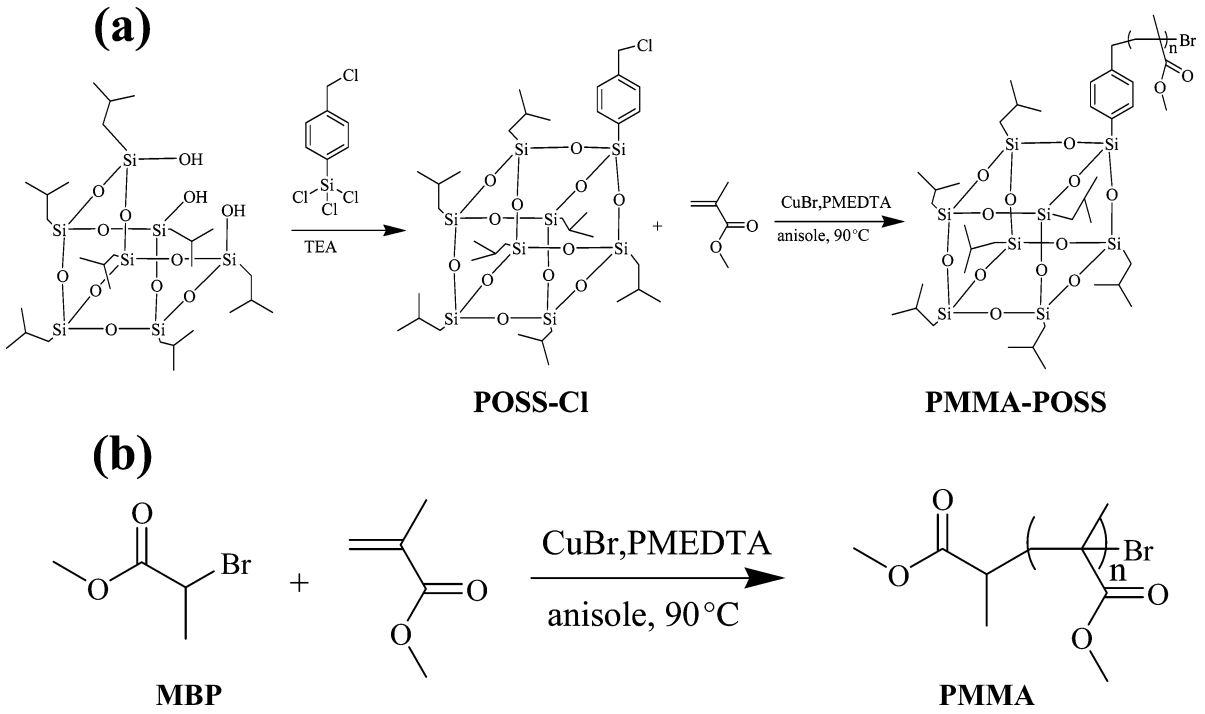

2-bromopropionate (MBP), triethylamine (TEA), and trichloro[4-(chloromethyl)phenyl]silane were all used as received. All solvents were distilled prior to use.

We used the corner-capping reaction to prepare POSS-Cl initiator in which only one corner is functionalized with an atom transfer radical polymerizable group (Scheme l). The initiator, POSS-Cl, was prepared by reacting trichloro[4-(chloromethyl)phenyl]silane (1.00 mL, 5.61 mmol) with isobutyltrisilanol-POSS (4.05 g, 5.11 mmol) in the presence of triethylamine (2.20 mL, 15 mmol) in 30.0 mL of dry THF under argon. The reaction flask was stirred at room temperature for 7.5 h, followed by filtration to remove the $HNEt_3$-Cl byproduct. The clear THF solution was dropped into a beaker of acetonitrile and rapidly stirred. The resulting product was collected by filtration and dried in a vacuum. (4.61 g, 80%). ^{1}H NMR ($CDCl_3$), δ: 7.59 (d, 2H), 7.33 (d, 2H), 4.52 (s, 2H), 1.92−1.62 (m, 7H), 1.09−0.85 (m, 42H), 0.75−0.48 (m, 14H).

Syntheses of Polymers. To prepare the PMMA−POSS homopolymers, the atom transfer radical polymerization with CuBr/PMDETA was carried out (Scheme 1).The molecular weights of PMMA−POSS (M_n = 10 350 g/mol and M_n = 29 700 g/mol) were determined by GPC. In accordance with the controlled polymerization characteristics of ATRP, the resulted LPMMA−POSS (M_n = 10 350 g/mol) homopolymer has narrow polydispersity (PDI = 1.15), and that of the HPMMA−POSS (M_n = 29 700 g/mol) has also a narrow molecular weight distribution (PDI = 1.18). Similarly, the PMMA homopolymers were also prepared by ATRP with methyl DL-2-bromopropionate monofunctional initiator. The molecular weights of PMMA (M_n = 9800 g/mol and M_n = 28 900 g/mol) were also determined by GPC. The polydispersity of the LPMMA (M_n = 9800 g/mol) and the HPMMA (M_n = 28 900 g/mol) are 1.15 and 1.17, respectively. The phenolic resins was synthesized with sulfuric acid via a condensation reaction and with average molecular weights of M_n = 500 g/mol and M_w = 1200 g/mol that was described in the previous study.[35] Chemical structures of PMMA and phenolic resin are shown in Scheme 2. Symbols and characterizations of these above-mentioned polymers are summarized in Table 1.

Blend Preparations. Desired composition containing PMMA or PMMA−POSS and phenolic was dissolved in THF at a concentration of 5 wt % and stirred for 6−8 h. The solution was allowed to evaporate slowly at 25 °C for 1 day on a Teflon plate and dried at 90 °C for 3 days to ensure total elimination of the solvent.

Differential Scanning Calorimetry (DSC). Thermal analysis was carried out on a DSC instrument from the DuPont (model 910 DSC-9000 controller) with a scan rate of 20 °C/min and a temperature range of 30−170 °C in a nitrogen atmosphere. An ∼5−10 mg sample was weighted and sealed in an aluminum pan. The sample was then quickly cooled to room temperature from the first scan and then scanned between 30 and 280 °C at a scan rate of 20 °C/min. The glass transition temperature is taken as the midpoint of the heat capacity transition between the upper and lower points of deviation from the extrapolated glass and liquid lines.

FT-IR and 2D-IR Spectra. FT-IR measurement was made using a Nicolet Avatar 320 FT-IR spectrometer; 32 scans at a resolution of 1 cm^{-1} were collected with a NaCl disk. The THF solution containing the sample was cast onto a NaCl disk and dried under condition similar to that used in bulk preparation. The sample chamber was purged with nitrogen in order to maintain the film dryness. 2D correlation analysis was performed using "Vertor 3D" software supplied by Bruker Instrument Co. All the spectra applied to the 2D-IR correlation analysis were normalized and negative intensities of auto peaks or cross-peaks in 2D-IR correlation spectra are indicated by shaded regions; positive intensities are indicated by unshaded regions. Synchronous 2D-IR spectra were used to study the specific interactions in these blends.

Results and Discussion

DSC Analyses. The conventional second run DSC thermogramsof LPMMA (M_n = 9800 g/mol) or LPMMA−POSS (M_n = 10 350 g/mol) and phenolic blends with various weight ratios are shown in parts a and b of Figure 1, respectively. All blends show a composition-dependent single T_g, indicating that these blends are all fully miscible. Generally, if the T_g−composition relationship is deviated obviously, neither a linear relationship nor the ideal rule of Fox is applicable.[36] It has been generally suggested that the T_g relationship to the composition of the miscible polymer blends follows the Kwei equation:[37]

$$T_g = \frac{W_1 T_{g1} + kW_2 T_{g2}}{W_1 + kW_2} + qW_1 W_2 \qquad (1)$$

where W_1 and W_2 are weight fractions of the components, T_{g1} and T_{g2} represent the corresponding glass transition temperatures,

Scheme 2. Schematic Diagram Showing Types of Interaction between PMMA and Phenolic

Phenolic Resin

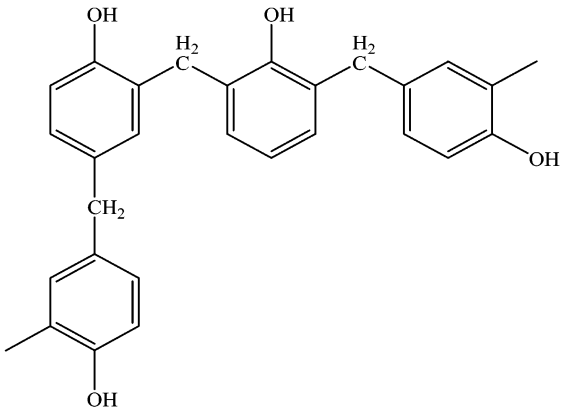

PMMA

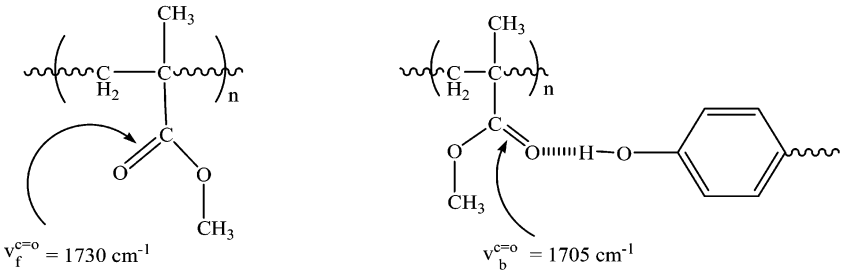

Table 1. Summary of Symbols and Characterizations of Polymers

polymers	initiator	M_n	PDI	T_g (°C)
LPMMA	MBP	9 800	1.15	117
LPMMA-POSS	POSS-Cl	10 350	1.15	120
HPMMA	MBP	28 900	1.17	119
HPMMA-POSS	POSS-Cl	29 700	1.18	122
phenolic		500	2.40	50

and k and q are fitting constants. The q is a parameter corresponding to the strength of specific interactions in the blend, reflecting a balance between the breaking of the self-association and the forming of the interassociation interactions. As shown in Figure 2, we can obtain $k = 1$ and $q = 35$ from phenolic/LPMMA−POSS blends and $k = 1$ and $q = -37$ from phenolic/LPMMA blends using the nonlinear least-squares "best fit" values. These phenolic/LPMMA−POSS blends resulted in positive deviation while phenolic/LPMMA blends result in negative deviation comparing with that predicted by linear rule, but both show positive deviation by the Fox rule. This result reveals that the incorporation a small amount of POSS on the PMMA chain end significantly shifts thermal properties of the phenolic/LPMMA blend due to stronger interassociation interaction exists between LPMMA−POSS and the phenolic resin than that of the phenolic/LPMMA. In higher molecular weight PMMA blend systems, the conventional second run DSC thermograms of HPMMA (M_n = 28 900 g/mol), HPMMA−POSS (M_n = 29 700 g/mol), and their blends with phenolic are shown in Figure 3a,b. Similarly, $k = 1$ and $q = 22$ for the phenolic/HPMMA−POSS blend and $k = 1$ and $q = -36$ for the phenolic/HPMMA blend were obtained on the basis of the Kwei equation, as shown in Figure 4. Again, the strong

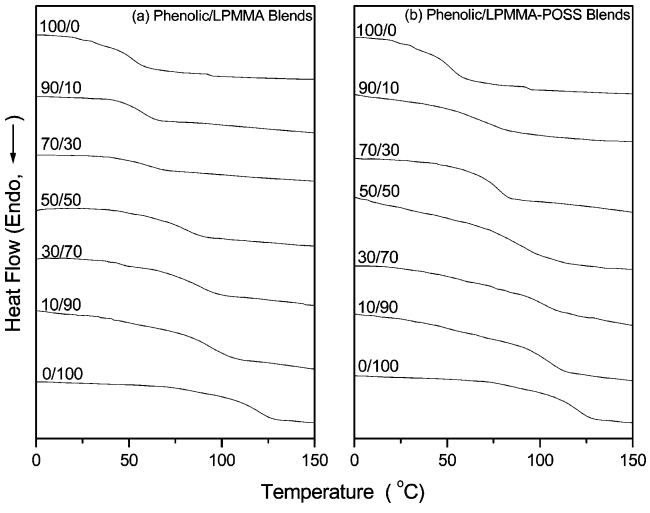

Figure 1. DSC thermograms of phenolic blends with either LPMMA or LPMMA−POSS with different compositions (weight ratio).

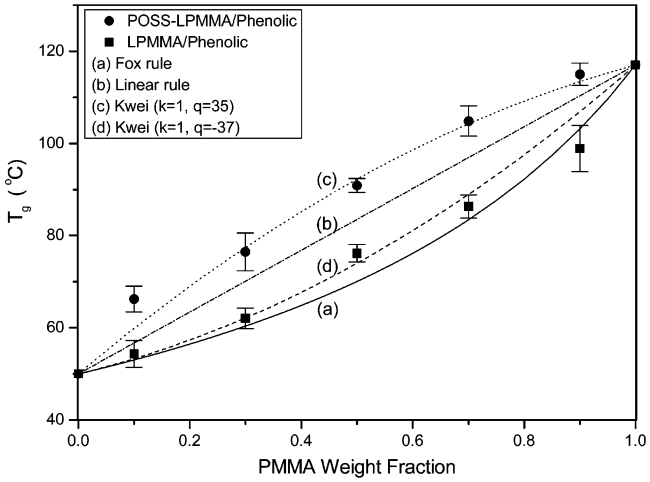

Figure 2. T_g vs composition curves based on (a) the Fox rule, (b) the linear rule, (c) the Kwei equation for the LPMMA−POSS system, and (d) the Kwei equation for LPMMA system: (●) experimental data of LPMMA−POSS blends; (■) experimental data of LPMMA blends.

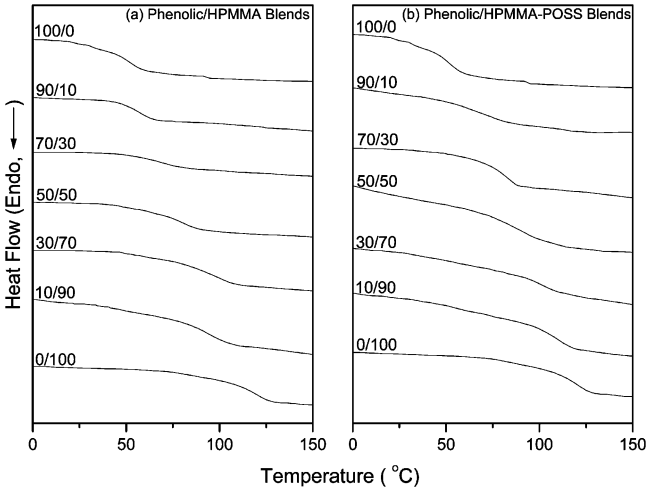

Figure 3. DSC thermograms of phenolic blends with either HPMMA or HPMMA−POSS with different compositions (weight ratio).

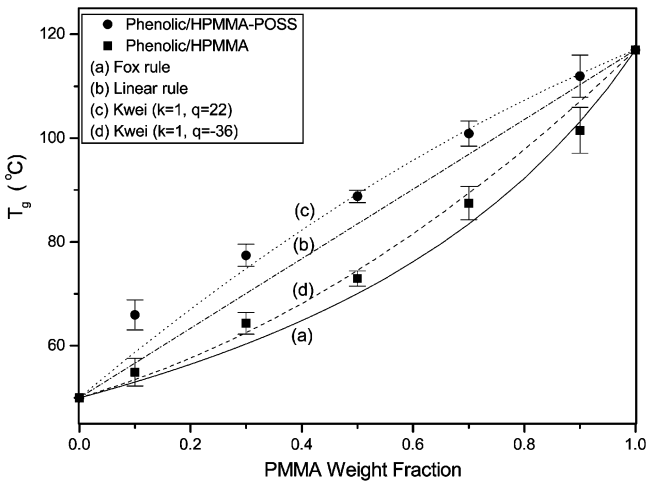

Figure 4. T_g vs composition curves based on (a) the Fox rule, (b) the linear rule, (c) the Kwei equation for HPMMA−POSS system, and (d) the Kwei equation for HPMMA system: (●) experimental data of HPMMA−POSS blends; (■) experimental data of HPMMA blends.

interassociation interaction between HPMMA−POSS and phenolic resin is responsible for the observed positive deviation, implying that the incorporation of the POSS chain end into the higher molecular weight PMMA also affects the interaction between PMMA and phenolic resin. We will quantitatively analyze this influence in later FT-IR analyses. The q value of phenolic/HPMMA blends is −36 and −37 for phenolic/LPMMA, indicating that the self-association interaction of the phenolic resin is stronger than the interassociation interaction between PMMA and phenolic resin while the effect of PMMA molecular weight is insignificant. The obtained results of the phenolic/PMMA blend are quite agreeable with previous literature.[19]

FT-IR Spectra. Chemical structures of PMMA and phenolic are shown in Scheme 2, showing IR vibrations of the free and hydrogen-bonded carbonyls of the PMMA with phenolic. Figure 5 shows the scale-expanded infrared spectra in the hydroxyl-stretching region of various compositions of phenolic/PMMA−POSS blends (Figure 5b,d) and phenolic/PMMA blends (Figure 5a,c) at room temperature. The spectrum of the pure phenolic resin shows a broad band at 3350 cm^{-1} and a shoulder at 3525 cm^{-1}, corresponding to the multimer hydrogen-bonded hydroxyl groups and the free hydroxyl groups, respectively. The intensity of the free hydroxyl bands decreases with the increase of the PMMA−POSS or the PMMA content in these blends. It is expected that great fraction of these "free" OH groups is consumed by forming the interassociation hydrogen bonds in these blends. In phenolic/PMMA blends, the band (at ca. 3420 cm^{-1}) appears with the increase of the PMMA content as the result of the decrease in the free hydroxyl band. Therefore, it is reasonable to assign this band at 3420 cm^{-1} as the hydroxyl group bonded to the carbonyl group. In addition, the spectra in the 2700−3700 cm^{-1} region from these blends with PMMA−POSS are broader and more asymmetric than the corresponding blends with PMMA. Meanwhile, we also observe a shoulder at 3325 cm^{-1}, corresponding to the hydroxyl−siloxane interaction.[39] This phenomenon depicts a new distribution of hydrogen-bonding formation resulting from the competition between hydroxyl−hydroxyl (3350 cm^{-1}), hydroxyl−carbonyl (3420 cm^{-1}), and hydroxyl−siloxane (3325 cm^{-1}) interactions. Coleman et al. compared the frequency difference ($\Delta\nu$) between the hydrogen-bonded hydroxyl absorption and the free hydroxyl absorption to access the average strength of the intermolecular interaction.[38] Therefore, the hydroxyl−hydroxyl self-interaction is clearly stronger than the hydroxyl−carbonyl interassociation from Figure 5a,c for phenolic/PMMA blends. These results are consistent with the negative q value of the phenolic/PMMA blend obtained from the Kwei equation. It is interesting to notice that the hydroxyl−siloxane interaction is even stronger than the hydroxyl−hydroxyl interaction and that is reasonable for the positive q value of phenolic/PMMA−POSS blends. The POSS moiety plays the role of nanocage to enhance the T_g with various content.[31] Now we turn our attention to Figure 5b,d, the spectra of Figure 5b corresponding to blends of LPMMA−POSS which are broader and more asymmetric than those blends with LPMMA. A shoulder corresponding to the hydroxyl−siloxane interaction appears at 3325 cm^{-1}, suggesting that competitive hydrogen-bonding formations exist between hydroxyl−hydroxyl, hydroxyl−carbonyl, and hydroxyl−siloxane, while the hydroxyl−siloxane is more favorable. The spectra of Figure 5d do not show the shoulder and asymmetric pattern, which is similar to the spectra of phenolic/HPMMA blends of Figure 5c, indicating that most hydrogen-bonding interactions come from the hydroxyl−carbonyl.

Figure 6 shows the infrared spectra of the carbonyl stretching measured at room temperature ranging from 1670 to 1780 cm^{-1} for different compositions of the phenolic/PMMA blends (Figure 6a,c) and phenolic/PMMA−POSS blends (Figure 6b,d). For the MMA unit, the IR carbonyl stretching absorptions by free and hydrogen-bonded carbonyl groups are at 1730 and 1705 cm^{-1}, respectively.[24] It clearly shows that the fraction of hydrogen-bonded carbonyl in the phenolic/PMMA system is greater than that of the phenolic/PMMA−POSS system as shown in Figure 6, especially in the lower molecular weight PMMA system. A routine procedure of least-squares curve fitting can be applied to the carbonyl stretching region using two Gaussian bands, and a quantitative measure of the fraction of "free" carbonyl groups can be readily determined using the value of absorptivity coefficient 1.5, which is the ratio of these two bands, the free and hydrogen-bonded carbonyl groups in an ester group.[40,41] The parameters of the infrared carbonyl band are summarized in Table 2, where the hydrogen-bonded carbonyl fraction of PMMA−POSS or PMMA increases with the increase of the phenolic content. According to Figure 6 and Table 2, we can determine that the fraction of hydrogen-bonded carbonyl under similar composition is in the order phenolic/LPMMA > phenolic/HPMMA ∼ phenolic/HPMMA−POSS > phenolic/LPMMA−POSS. Indeed, the PMMA tethered with POSS chain-

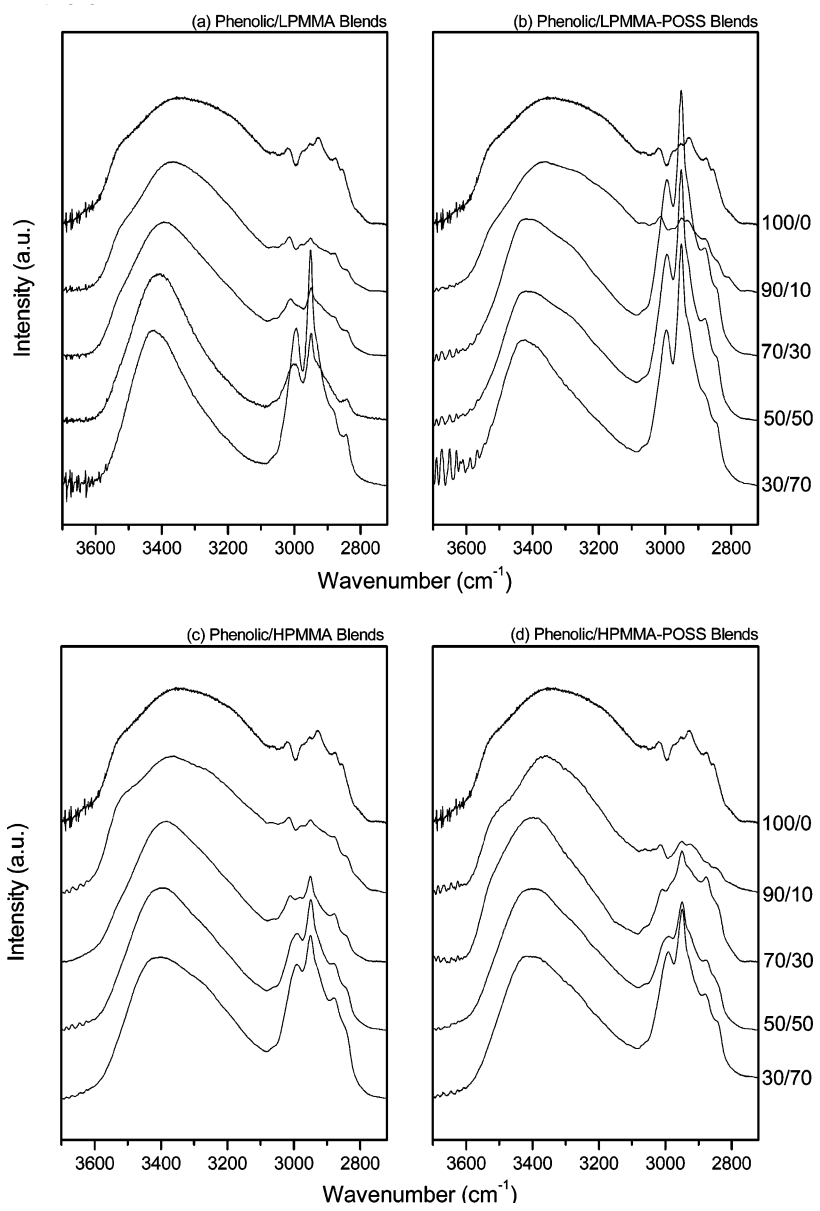

Figure 5. FT-IR spectra recorded at room temperature in the 2700−3700 cm^{-1} region of phenolic blends with either PMMA or PMMA−POSS with different compositions (weight ratio).

end changes the interaction between phenolic and PMMA, especially in lower molecular weight PMMA systems.

2D-IR Correlation Analyses. To further understand the influence on T_g and the order of the hydrogen-bonded carbonyl fraction in these POSS-containing polymer hybrids, the characterization of 2D-IR correlation spectra of these blends was carried out. Figure 7a−c shows the synchronous 2D-IR correlation maps of phenolic/PMMA and phenolic/PMMA−POSS blends in the range of 1200−1800 cm^{-1}. The molecular weight of PMMA shown in Figure 7 is about 10 000 g/mol. Bands in Figure 7a are mainly 1750 cm^{-1} for the carbonyl group of PMMA and 1510 cm^{-1} for the phenyl-OH group of the phenolic resin. Two strong auto- and cross-peaks appear between 1510 and 1750 cm^{-1}, indicating the specific interactions between these two groups. Figure 7c shows the effect of POSS presence where the intensity of auto- and cross-peak at 1510 cm^{-1} from the phenyl-OH group of the phenolic resin becomes weaker after the POSS incorporating into the chain end of PMMA. This result demonstrates that the bulky POSS end group may play a physical constraint for the conformation of the phenolic resin. Therefore, the flipping motions of phenyl-OH rings on the phenolic resin have a larger external perturbation angular frequency (∼180°). The reduced cross-correlation function ($X(\tau)$) was proposed by Noda:[25]

$$X(\tau) = \Phi(\nu_1,\nu_2)\cos(\omega\tau) + \Psi(\nu_1,\nu_2)\sin(\omega\tau) \qquad (2)$$

In eq 2, the terms, $\Phi(\nu_1,\nu_2)$ and $\Psi(\nu_1,\nu_2)$ are regarded as the real and imaginary parts of the function and are referenced as the cross-peak intensities in asynchronous and synchronous correlation maps. ω is the external perturbation angular frequency. In the case of $\omega = 180$, the $\cos(\omega\tau)$ equals zero and $\sin(\omega\tau)$ equals −1.0. Therefore, we expect to obtain the weakest cross-peak intensity in synchronous correlation maps.

Peaks corresponding to the Si−O−Si group of the POSS shown in parts b and c of Figure 7 are at 1250 and 1100 cm^{-1}, respectively. Both of these peaks possess a weak autopeak, indicating that the presence of POSS is in very low concentration in these blends. The entanglement molecular weight of PMMA is ca. 20 000 g/mol.[42,43] In the following case, as shown in Figure 8a,b, we demonstrate the behavior of POSS in the phenolic/PMMA blend in which the molecular weight of PMMA is above

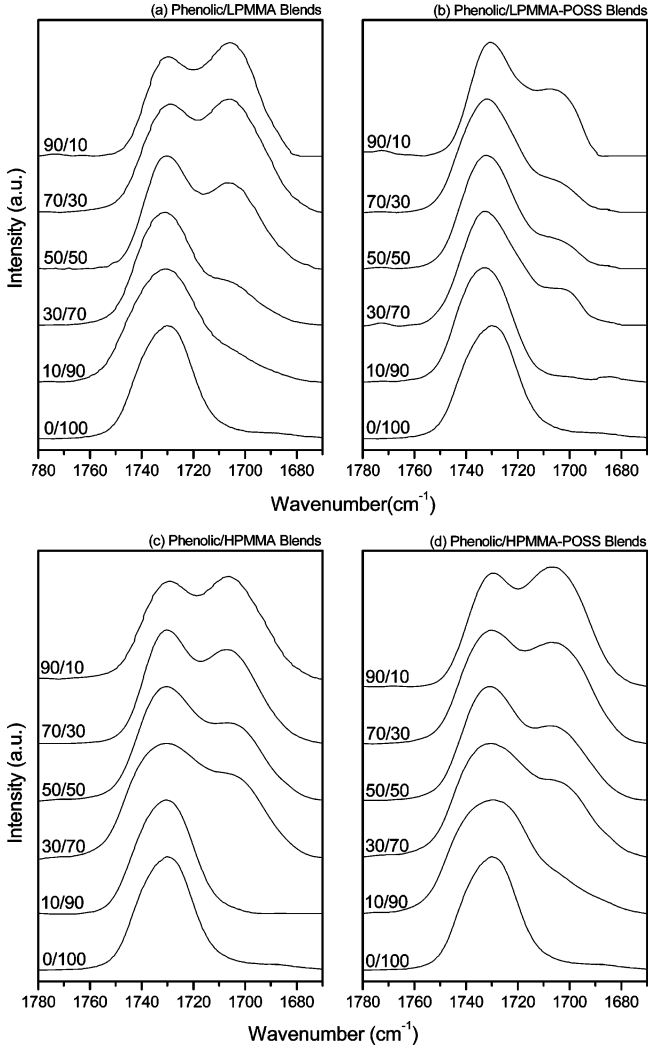

Figure 6. FT-IR spectra recorded at room temperature in the 1675−1780 cm^{-1} region of phenolic blends with either PMMA or PMMA−POSS with different compositions (weight ratio).

its entanglement molecular weight at about 30 000 g/mol. Figure 8a has a similar pattern as Figure 7a but shows stronger cross-peaks at several positions: 1750−1510, 1420, and 1510−1200 cm^{-1}. The 1200 and 1420 cm^{-1} correspond to the methyl group and the C−O of PMMA, respectively. Figure 8b also has a similar pattern as Figure 7b. This observation indicates that increasing of the molecular weight of PMMA gives greater interassociation interaction of hydroxyl−carbonyl in the phenolic/PMMA blend, similar to above-mentioned results. The incorporation of POSS into PMMA as chain end tends to decrease the interassociation interaction of the hydroxyl−carbonyl between PMMA and phenolic resin from the relatively lower molecular weight of PMMA. When the molecular weight of PMMA is above its entanglement molecular weight, the effect of POSS on the interassociation interaction of hydroxyl−carbonyl between PMMA and phenolic resin becomes insignificant.

Specific Interactions Analyses. In our previous study,[4,39] we have confirmed the existence of a specific interaction between the siloxane of the POSS moiety and the hydroxyl of the phenolic. To further investigate the above-mentioned phenomenon, an association model extended to ternary component system has been applied to this phenolic/PMMA−POSS blend. According to the Painter−Coleman association model (PCAM),[21] we designate B, A, and C as phenolic, PMMA, and POSS,

Table 2. Carbonyl Group Curve-Fitting Results of the PMMA or Phenolic/PMMA−POSS Blends with Two Different Molecular Weights[a]

	free C=O		H-bonded C=O		
samples (wt %)	ν_f (cm^{-1})	A_f (%)	ν_b (cm^{-1})	A_b (%)	f_b[a] (%)
phenolic/LPMMA					
30/70	1730	69.3	1705	30.7	22.7
50/50	1730	58.1	1705	41.9	32.4
70/30	1730	46.1	1705	53.9	44.9
90/10	1730	34.7	1705	65.3	55.6
phenolic/LPMMA−POSS					
30/70	1730	78.6	1705	21.4	15.3
50/50	1730	71.3	1705	28.7	21.1
70/30	1730	64.7	1705	35.3	26.6
90/10	1730	58.3	1705	41.7	32.3
phenolic/HPMMA					
30/70	1730	68.3	1705	31.7	23.5
50/50	1730	57.7	1705	42.3	32.8
70/30	1730	52.7	1705	47.3	38.6
90/10	1730	39.9	1705	60.1	52.1
phenolic/HPMMA−POSS					
30/70	1730	74.7	1705	25.3	18.4
50/50	1730	62.4	1705	37.6	28.6
70/30	1730	51.4	1705	48.6	37.6
90/10	1730	40.0	1705	60.0	50.3

[a] ν_f = wavenumber of free C=O of PMMA, ν_b = wavenumber of hydrogen-bonded carbonyl of PMMA, A_f = free C=O area fraction of PMMA, A_b = C=O area fraction of hydrogen-bonded PMMA, and f_b = fraction of hydrogen-bonded PMMA = $(A_b/1.5)/(A_b/1.5 + A_f)$.

respectively, and K_2, K_B, K_A, and K_C as their corresponding association equilibrium constants.

$$B_1 + B_1 \overset{K_2}{\longleftrightarrow} B_2 \tag{3}$$

$$B_h + B_1 \overset{K_B}{\longleftrightarrow} B_{h+1}\ (h \geq 2) \tag{4}$$

$$B_h + C_1 \overset{K_c}{\longleftrightarrow} B_hC \tag{5}$$

$$B_h + A_1 \overset{K_A}{\longleftrightarrow} B_hA \tag{6}$$

These four equilibrium constants can be expressed as follows in terms of volume fractions

$$\Phi_B = \Phi_{B1}\Gamma_2\left[1 + \frac{K_A\Phi_{A1}}{r_A} + \frac{K_C\Phi_{C1}}{r_C}\right] \tag{7}$$

$$\Phi_A = \Phi_{A1}[1 + K_A\Phi_{B1}\Gamma_1] \tag{8}$$

$$\Phi_C = \Phi_{C1}[1 + K_C\Phi_{B1}\Gamma_1] \tag{9}$$

where

$$\Gamma_1 = \left(1 - \frac{K_2}{K_B}\right) + \frac{K_2}{K_B}\left(\frac{1}{1 - K_B\Phi_{B1}}\right) \tag{10}$$

$$\Gamma_2 = \left(1 - \frac{K_2}{K_B}\right) + \frac{K_2}{K_B}\left(\frac{1}{(1 - K_B\Phi_{B1})^2}\right) \tag{11}$$

Φ_B, Φ_A, and Φ_C are the volume fractions of repeat units in the blend, Φ_{B1}, Φ_{A1}, and Φ_{C1} are the volume fractions of isolated units in the blend, and $r_A = V_A/V_B$ and $r_C = V_C/V_B$ are the ratios of segmental molar volumes.

The self-association constants of phenolic resin ($K_2 = 23.3$ and $K_B = 52.3$) and the interassociation constant between phenolic resin and POSS ($K_C = 38$) have been determined in

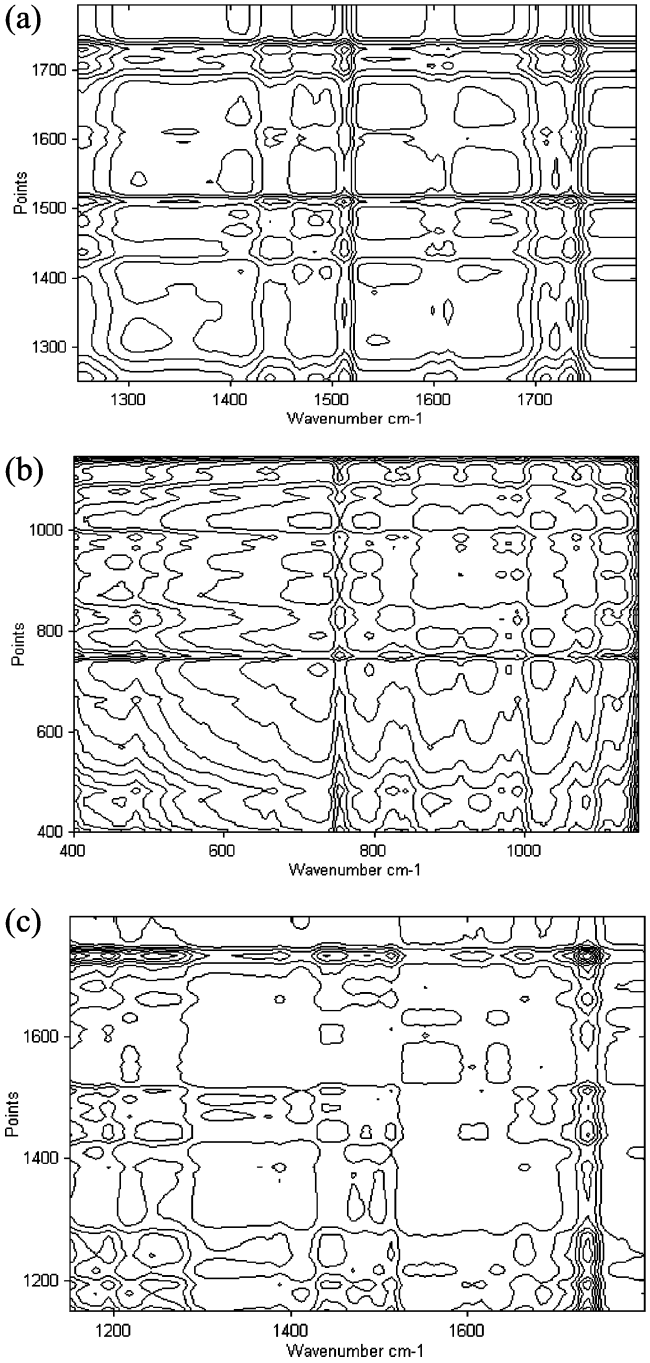

Figure 7. Synchronous 2D correlation map for (a) phenolic/LPMMA blends in the region from 1200 to 1800 cm^{-1}, (b) phenolic/LPMMA−POSS blends in the region from 400 to 1200 cm^{-1}, and (c) phenolic/LPMMA−POSS blends in the region from 1100 to 1800 cm^{-1}.

our previous study.[4] The interassociation constant K_A value is determined directly from a least-squares fitting procedure based on the fraction of hydrogen-bonded carbonyl experimentally obtained in the binary phenolic/PMMA blend. In this phenolic/HPMMA blend, the interassociation constant ($K_A = 16$) obtained is same as our previous study.[19] However, when the PMMA molecular weight is lower than the entanglement molecular weight, we obtain a higher interassociation constant in the phenolic/LPMMA blend ($K_A = 20$) than that in the phenolic/HPMMA blend ($K_A = 16$). The smaller molecular weight PMMA contains a greater fraction of the hydrogen-bonded carbonyl that may come from the greater entropy change and resulted in better miscibility based on thermodynamic reasons.[44] Table 3 lists all the parameters required by the Painter−Coleman

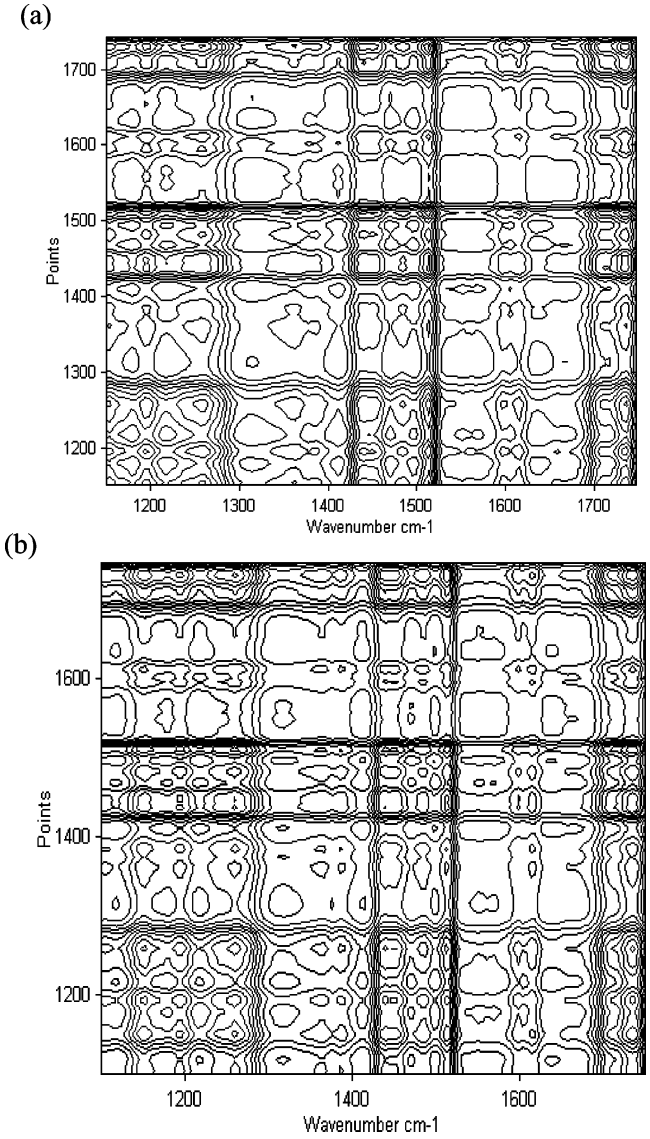

Figure 8. Synchronous 2D correlation map for (a) phenolic/HPMMA blends in the region from 1100 to 1800 cm^{-1} and (b) phenolic/HPMMA−POSS blends in the region from 1100 to 1800 cm^{-1}.

Table 3. Summary of the Self-Association and Interassociation Equilibrium Constants and Thermodynamic Parameter of Phenolic/PMMA and Phenolic/PMMA−POSS Blends at 25 °C[a]

				equilibrium constant			
polymer	V	MW	DP	K_2	K_B	K_A[c]	K_C[d]
phenolic[b]	84	105	6	23.3	52.3		
LPMMA	84.9	100	90			20	
HPMMA	84.9	100	280			16	
POSS	778.6	872.2	1				38

[a] V = molar volume (mL/mol), MW = molecular weight (g/mol), δ = solubility parameter $(cal/mL)^{1/2}$, DP = degree of polymerization, K_2 = dimer self-association equilibrium constant, K_B = multimer self-association equilibrium constant, and K_A = interassociation equilibrium constant. [b] Reference 35. [c] Calculated by the PCAM model in this study. [d] Reference 4.

association model to estimate thermodynamic properties for these blends. If we know these equilibrium constants (K_2, K_B, K_C, K_A) and segment molar volumes, the fraction of hydrogen-bonded carbonyl group can be calculated from eqs 7−11 using

$$f_{HB} = 1 - \frac{\Phi_{C1}}{\Phi_C} \tag{12}$$

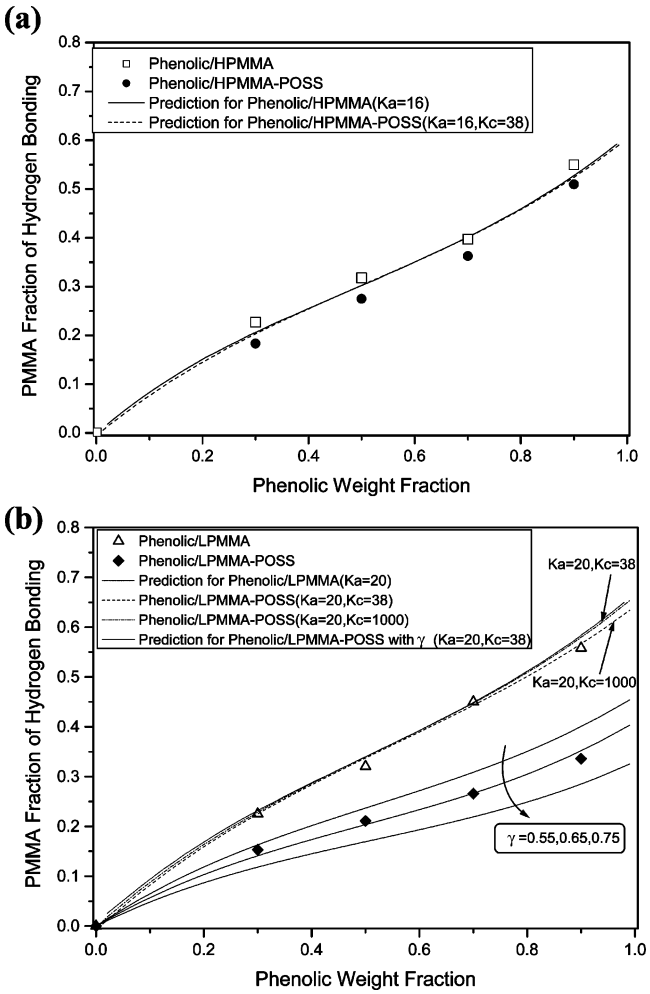

Figure 9. PMMA and PMMA−POSS fraction of hydrogen-bonded carbonyl vs phenolic content for blends from FT-IR spectra.

Therefore, the predicted fraction of hydrogen bonding of carbonyl groups shown in Figure 9 can be calculated numerically.

Figure 9 plots the experimental data and the prediction curves by using the PCAM model of PMMA and PMMA−POSS vs the phenolic weight fraction of these four blend systems from the FT-IR of hydrogen-bonded carbonyl region. In these phenolic/PMMA blends, the experimental data are quite agreeable with the prediction from the PCAM model, which are similar to our previous study.[19] It is worth noting that there is a large deviation from PCAM prediction curve ($K_A = 20$, $K_C = 38$) in phenolic/LPMMA−POSS blends shown in Figure 9b but gives only a relatively smaller deviation from PCAM prediction curve ($K_A = 16$, $K_C = 38$) in phenolic/LPMMA blends. It is interesting to know which parameter based on PCAM is more important to affect the fraction of hydrogen-bonded carbonyl group. In this case, K_2 and K_B are calculated on the basis of model compounds, K_A is calculated from the hydrogen-bonded carbonyl group of the binary phenolic/PMMA blend, and these parameters are supposed to be constant. Therefore, if the K_C value becomes larger, such as $K_C = 1000$, the predicted curve in Figure 9b should also give a larger deviation in this phenolic/LPMMA−POSS blend system. It is reasonable because the POSS content in the LPMMA−POSS homopolymer is below 10 wt %, so the contribution to compete hydrogen bonding with the carbonyl is relatively insignificant. By considering these above-mentioned differences, other factors such as chain connectivity, flexibility, and architecture may also

Scheme 3. Proposed Screening Effect Microstructure in Phenolic/PMMA−POSS Blends

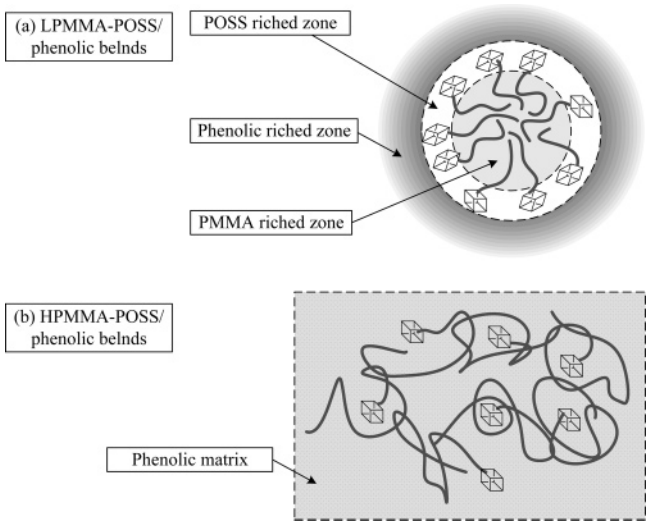

play important roles to a certain extent according to earlier literature.[45] A parameter, γ, was introduced and defined as the fraction of same chain contacts originating from the polymer chain self-bending, primarily through local but also through long-range connectivity effects. The equilibrium constants in eqs 7 and 8 can be redefined as[45]

$$\tilde{K}_B = K_B\left[\frac{\gamma + (1-\gamma)\Phi_B}{\Phi_B}\right] \quad (13)$$

$$\tilde{K}_A = K_A\left[\frac{1-(\gamma + (1-\gamma)\Phi_B)}{\Phi_A}\right] = K_A(1-\gamma) \quad (14)$$

These equations are obtained by defining the probability of a B group being next to a B group, i.e.

$$p_{BB} = \gamma + (1-\gamma)\Phi_B \quad (15)$$

where γ is the fraction of intrachain contacts as mentioned above and $(1-\gamma)\Phi_B$ is a measure of interchain contacts. The probability of an AB contact, p_{AB}, is then simply $(1 - p_{BB})$. Figure 9b compares the experimental data with the predicted curves calculated using γ values of 0.55, 0.65, and 0.75. The γ value of 0.65 results in the best agreement between prediction and experiment, implying that about 65% of intrachain with POSS tethered contacts along LPMMA chain. Here, we propose a schematic representation for the phenolic/PMMA−POSS blend in Scheme 3. The chain structure of the LPMMA−POSS acts as a macromolecular surfactant due to lack of entanglement in the LPMMA chain. The POSS and PMMA segment function as hydrophilic and hydrophobic sites, respectively. Further comparison of interassociation equilibrium constant in each functional group, it depicts that the interassociation equilibrium constant between phenolic hydroxyl and POSS siloxane is greater than the interassociations equilibrium constant of hydroxyl and carbonyl at room temperature. By blending the LPMMA−POSS with phenolic resin matrix, a micelle structure with the POSS shell and the PMMA core is expected as shown in Scheme 3a. This phenomenon can be rationalized by the so-called "screening effect" in phenolic/LPMMA−POSS blends because the interassociation equilibrium constant between hydroxyl and POSS is greater than the interassociation equilibrium constant between hydroxyl and carbonyl. This also manifests why no deviation has been observed between the

experimental data and the prediction curves in the phenolic/LPMMA−POSS blend. This γ value of 0.65 is lower than the EPh/dendrimer-like polyester blend ($\gamma = 0.8$)[46] but higher than the EMAVPh/PEO blend system ($\gamma = 0.3$),[47] suggesting that the chain structure is somewhat between the dendrime-like and linear chain structures. In the phenolic/HPMMA−POSS blends (Scheme 3b) where the molecular weight of PMMA is above its entanglement molecular weight, the PMMA chain are randomly distributed within the phenolic matrix, and the contribution of the POSS competing hydrogen bond with the carbonyl group of PMMA becomes less, similar to that in the binary phenolic/HPMMA blend. As mentioned above in Figure 5b,d, the analyses of this figure are consistent with our proposed Scheme 3, while the hydroxyl−siloxane is more favorable in phenolic/LPMMA−POSS; however, the phenolic/HPMMA−POSS is favored in hydroxyl−carbonyl.

Conclusions

A series of phenolic/PMMA−POSS and PMMA blends have been prepared and investigated by DSC, FT-IR, and 2D-IR. All these blends are totally miscible in the amorphous phase over entire compositions. Among these blends, single T_gs of the phenolic/PMMA−POSS blends with positive q value were observed and higher than that of the phenolic/PMMA blends with negative q value. The positive deviation of the phenolic/PMMA−POSS blend reveals that a strong interassociation interaction exists between POSS siloxane and phenolic hydroxyl. FT-IR analysis indicates that the PMMA chain of the LPMMA−POSS cannot form entanglement with lower hydrogen-bonding interaction between LPMMA and phenolic resin. Furthermore, we found a "screening effect" in these phenolic/LPMMA−POSS blends caused by the POSS chain end tethered, which has the greater interassociations equilibrium constant between hydroxyl and POSS than the interassociations equilibrium constant between hydroxyl and carbonyl. On the contrary, the molecular weight of HPMMA−POSS chain is above its entanglement molecular weight; the hydrogen bonding between POSS and hydroxyl becomes less than that between PMMA and hydroxyl.

Acknowledgment. This research was financially supported by the National Science Council, Taiwan, Republic of China, under Contract NSC-93-2216-E-009-021.

References and Notes

(1) Novak, B. M. *Adv. Mater.* **1993**, *5*, 442.
(2) Tamaki, R.; Chujo, Y.; Kuraoka, K.; Yazawa, T. *J. Mater. Chem.* **1999**, *8*, 1741.
(3) Chujo, Y.; Kure, S.; Matsuki, H.; Saegusa, T. *Polym. Prepr. Jpn.* **1993**, *42*, 839.
(4) Lee, Y. J.; Kuo, S. W.; Huang, W. J.; Lee, H. Y.; Chang, F. C. *J. Polym. Sci., Part B: Polym. Phys.* **2004**, *42*, 1127.
(5) Zhang, W.; Fu, B. X.; Seo, Y.; Schrag, E.; Hsiao, B.; Mather, P. T.; Yang, N. L.; Xu, D.; Ade, H.; Rafailovich, M.; Sokolov, J. *Macromolecules* **2002**, *35*, 8029.
(6) Zheng, L.; Kasi, R. M.; Farris, R. J.; Coughlin, E. B. *J. Polym. Sci., Part A: Polym. Chem.* **2002**, *40*, 885.
(7) Fu, B. X.; Lee, A.; Haddad, T. S. *Macromolecules* **2004**, *37*, 5211.
(8) Lichtenhan, J. D.; Otonari, Y. A.; Carr, M. J. *Macromolecules* **1995**, *28*, 8435.
(9) Haddad, T. S.; Lichtenhan, J. D. *Macromolecules* **1996**, *29*, 7302.
(10) Kopesky, E. T.; Haddad, T. S.; Cohen, R. E.; McKinley, G. H. *Macromolecules* **2004**, *37*, 8992.
(11) Lee, A.; Lichtenhan, J. D. *Macromolecules* **1998**, *31*, 4970.
(12) Li, G. Z.; Wang, L.; Toghiani, H.; Daulton, T. L.; Koyama, K.; Pittman, C. Y. *Macromolecules* **2001**, *34*, 8686.
(13) Chen, W. Y.; Wang, Y. Z.; Kuo, S. W.; Huang, C. F.; Tung, P. H.; Chang, F. C. *Polymer* **2004**, *45*, 6897.
(14) Strachota, A.; Kroutilova, T.; Kovarova, J.; Matejka, L. *Macromolecules* **2004**, *37*, 9457.
(15) Matejka, L.; Strachota, A.; Plestil, J.; Whelan, P.; Steinhart, M.; Slouf, M. *Macromolecules* **2004**, *37*, 9449.
(16) Tsuchida, A.; Bolln, C.; Sernetz, F. G.; Frey, H.; Muhlhaupt, R. *Macromolecules* **1997**, *30*, 2818.
(17) Waddon, A. J.; Zheng, L.; Farris, R. J.; Coughlin, E. B. *Nano Lett.* **2002**, *2*, 1149.
(18) Tamaki, R.; Choi, J.; Laine, R. M. *Chem. Mater.* **2003**, *15*, 793.
(19) Huang, C. F.; Kuo, S. W.; Lin, H. C.; Chen, J. K.; Chen, Y. K.; Xu, H. Y.; Chang, F. C. *Polymer* **2004**, *45*, 5913.
(20) Zhang, X. Q.; Soloman, D. H. *Macromolecules* **1994**, *27*, 4919.
(21) Coleman, M. M.; Graf, J. F.; Painter, P. C. *Specific Interactions and the Miscibility of Polymer Blends;* Technomic Publishing: Lancaster, PA, 1991.
(22) Hill, D. J. T.; Whittaker, A. K.; Wong, K. W. *Macromolecules* **1999**, *32*, 5285.
(23) Kim, J. H.; Min, B. R.; Kim, C. K.; Won, J.; Kang, Y. S. *J. Phys. Chem. B* **2002**, *106*, 2786.
(24) Kuo, S. W.; Chang, F. C. *Macromolecules* **2001**, *34*, 4089.
(25) Noda, I. *J. Am. Chem. Soc.* **1989**, *111*, 8116.
(26) Zhang, J.; Duan, Y.; Shen, D.; Yan, S.; Noda, I.; Ozaki, Y. *Macromolecules* **2004**, *37*, 3292.
(27) Huang, H.; Malkov, S.; Coleman, M. M.; Painter, P. C. *Macromolecules* **2003**, *36*, 8148.
(28) Nakashima, K.; Ren, Y.; Nishioka, T.; Tsubahara, N.; Noda, I.; Ozaki, Y. *Macromolecules* **1999**, *32*, 6307.
(29) Huang, H.; Malkov, S.; Coleman, M. M.; Painter, P. *Macromolecules* **2003**, *36*, 8156.
(30) Lee, Y. J.; Huang, J. M.; Kuo, S. W.; Lu, J. S.; Chang, F. C. *Polymer* **2005**, *46*, 173.
(31) Xu, H. Y.; Kuo, S. W.; Lee, J. S.; Chang, F. C. *Macromolecules* **2002**, *35*, 8788.
(32) Xia, J. H.; Gaynor, S. G.; Matyjaszewski, K. *Macromolecules* **1998**, *31*, 5989.
(33) Haddleton, D. M.; Kukulj, D.; Duncalf, D. J.; Heming, A. J.; Shooter, A. J. *Macromolecules* **1998**, *31*, 5201.
(34) Patten, T. E.; Xia, J.; Abernathy, T.; Matyjaszewski, K. *Science* **1996**, *272*, 866.
(35) Wu, H. D.; Chu, P. P.; Ma, C. C. M.; Chang, F. C. *Macromolecules* **1999**, *32*, 3097.
(36) Fox, T. G. *Bull. Am. Phys. Soc.* **1956**, *2*, 123.
(37) Kwei, T. K. *J. Polym. Lett. Ed.* **1984**, *22*, 307.
(38) Moskala, E. J.; Varnell, D. F.; Coleman, M. M. *Polymer* **1985**, *26*, 228.
(39) Xu, H. Y.; Kuo, S. W.; Lee, J. S.; Chang, F. C. *Polymer* **2002**, *43*, 5117.
(40) Cortazar, M.; Pomposo, J. A. *Macromolecules* **1994**, *27*, 252.
(41) Serman, C. J.; Painter, P. C.; Coleman, M. M. *Polymer* **1991**, *32*, 1049.
(42) Lin, Y. H.; Juang, J. H. *Macromolecules* **1999**, *32*, 181.
(43) Krevelen, D. W. V.; Hoftyzer, P. J. *Properties of Polymers: Their Estimation and Correlation with Chemical Structure*; Elsevier Scientific Publishing: Amsterdam, 1976.
(44) Coleman, M. M.; Xu, Y.; Painter, P. C. *Macromolecules* **1994**, *27*, 127.
(45) Coleman, M. M.; Painter, P. C. *Macromol. Chem. Phys.* **1998**, *199*, 1307.
(46) Pruthtikul, R.; Coleman, M. M.; Painter, P. C.; Tan, N. B. *Macromolecules* **2002**, *34*, 4145.
(47) Painter, P. C.; Veytsman, B.; Kumar, S.; Shenoy, S.; Graf, J. F.; Xu, Y.; Coleman, M. M. *Macromolecules* **1997**, *30*, 932.

MA051923N